

IL NUOVO CIMENTO  
DOI 10.1393/ncc/i2005-10164-7

VOL. 28 C, N. 4-5

Luglio-Ottobre 2005

## Performance of GRB monitor with Astro-E2 Hard X-ray Detector (HXD-II)(\*)

S. HONG<sup>(1)(2)</sup>, K. YAMAOKA<sup>(3)</sup>, Y. TERADA<sup>(2)</sup>, M. OHNO<sup>(4)</sup>, A. TSUTSUI<sup>(3)</sup>  
Y. ENDO<sup>(1)</sup>, J. KOTOKU<sup>(5)</sup>, Y. OKADA<sup>(6)</sup>, M. MORI<sup>(1)</sup>, Y. FUKAZAWA<sup>(4)</sup>  
T. KAMAE<sup>(7)</sup>, M. KOKUBUN<sup>(6)</sup>, K. MAKISHIMA<sup>(6)(2)</sup>, T. MURAKAMI<sup>(8)</sup>  
K. NAKAZAWA<sup>(9)</sup>, M. NOMACHI<sup>(10)</sup>, M. TASHIRO<sup>(1)</sup>, I. TAKAHASHI<sup>(6)</sup>  
T. TAKAHASHI<sup>(9)</sup>, D. YONETOKU<sup>(8)</sup>, S. WATANABE<sup>(9)</sup> and THE HXD-II TEAM

<sup>(1)</sup> Department of Physics, Saitama University, Japan

<sup>(2)</sup> Institute of Physical and Chemical Research, Japan

<sup>(3)</sup> Department of Physics and Mathematics, Aoyama Gakuin University, Japan

<sup>(4)</sup> Department of Physical Sciences, Hiroshima University, Japan

<sup>(5)</sup> Department of Physics, Tokyo Institute of Technology, Japan

<sup>(6)</sup> Department of Physics, University of Tokyo, Japan

<sup>(7)</sup> Stanford Linear Accelerator Center, CA, USA

<sup>(8)</sup> Department of Physics, Kanazawa University, Japan

<sup>(9)</sup> Institute of Space and Astronautical Science, Japan Aerospace Exploration Agency, Japan

<sup>(10)</sup> Laboratory of Nuclear Physics, Osaka University, Japan

(ricevuto il 23 Maggio 2005; pubblicato online il 20 Ottobre 2005)

**Summary.** — The Hard X-ray Detector (HXD-II) is one of the three instruments onboard the *Astro-E2* satellite scheduled for launch in 2005. The HXD-II consists of 16 main counters (Well units), surrounded by 20 active shield counters (Anti units). The Anti units have a large geometrical area of  $\sim 800 \text{ cm}^2$  with an uncollimated field of view covering  $\sim 2\pi$  steradian. Utilizing 2.6 cm thick BGO crystals, they realize a large effective area of  $400 \text{ cm}^2$  for 1 MeV photons. In the energy range of 300–5000 keV, the expected effective area is significantly larger than those of other gamma-ray burst instruments, such as *CGRO/BATSE*, *HETE-2/FREGATE*, and *GLAST/GBM*. Therefore, the Anti units act as a Wideband All-sky Monitor (WAM) for gamma-ray bursts in the energy range of 50–5000 keV.

PACS 98.70.Rz –  $\gamma$ -ray sources;  $\gamma$ -ray bursts.

PACS 95.55.Ka – X- and  $\gamma$ -ray telescopes and instrumentation.

PACS 01.30.Cc – Conference proceedings.

### 1. – The Hard X-ray Detector onboard Astro-E2

*Astro-E2* is the fifth Japanese cosmic X-ray satellite scheduled for launch in 2005. This is a recovery mission to *Astro-E* that was lost in February 2000 due to a launch failure.

---

(\*) Paper presented at the “4th Workshop on Gamma-Ray Burst in the Afterglow Era”, Rome, October 18-22, 2004.

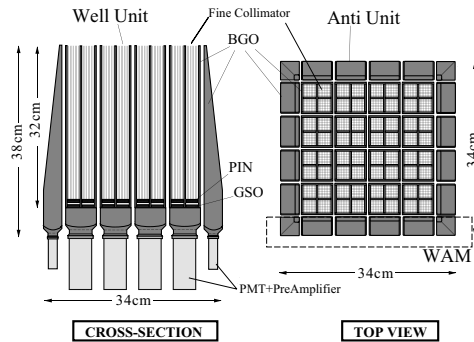


Fig. 1. – The schematic view of the HXD-II sensor.

There are three detector instruments onboard *Astro-E2*; the X-Ray Spectrometer (XRS) utilizing micro-calorimeter arrays, the X-ray Imaging Spectrometer (XIS) consisting of four X-ray CCD cameras, and the Hard X-ray Detector (HXD-II). The former two are placed on focal planes of the X-Ray Telescope (XRT).

The HXD-II is a non-imaging phoswich-type scintillation counter array, which covers an energy band of 10–600 keV. The counter array consists of 16 main units of well-type GSO ( $\text{Gd}_2\text{SiO}_5$ )/BGO ( $\text{Bi}_4\text{Ge}_3\text{O}_{12}$ ) phoswich counters (Well units), and 20 active shield units of thick BGO crystals (Anti units) which surround the Well units (see fig. 1). With the anti-coincidence method, background events caused by cosmic rays or Compton-scattered photons are dramatically reduced [1-3]. Further employing a tightly collimated field of view by the well-type phoswich configuration and passive collimators, the HXD-II realizes an extreme low background level of a few times  $10^{-5}$  counts/s/cm<sup>2</sup>/keV at 200 keV.

## 2. – Description of Anti units

The main purpose of the Anti units is to provide passive and active shields to the Well units. At the same time, they work as a Wideband All-sky Monitor (WAM) owing to the

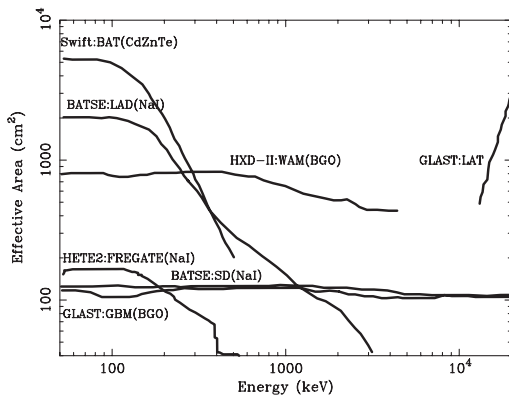


Fig. 2

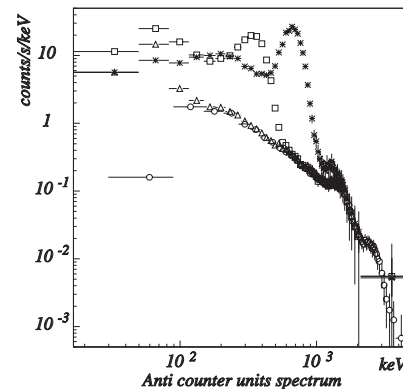


Fig. 3

Fig. 2. – The on-axis effective area of the WAM for one side, in comparison with those of other wide-field gamma-ray instruments.

Fig. 3. – The WAM spectra of  $^{133}\text{Ba}$  (square),  $^{241}\text{Am}$  (triangle) and  $^{137}\text{Cs}$  (star), compared with the background (circle). Each spectrum is a sum over 4 units of one side.

TABLE I. – *The GRB triggering parameters.*

	AE <sup>1</sup>	DE <sup>2</sup>
energy band	1 band in 4 band	2 free band
judge time	1 or 1/4 s	1 s
judge level	$16\sqrt{k/m}$ , $k, m = 1, 2, 4, 8$	0.025 – 63.75
integration time	8 s	1 – 8 s

<sup>(1)</sup>Analog electronics triggers for the GRB data acquisition.

<sup>(2)</sup>Digital electronics triggers with an onboard software.

following characteristics [4, 5]. First, by definition, the Anti units cover about half the whole sky. Second, these units have a large geometrical area reaching  $\sim 800 \text{ cm}^2$  per one of the four sides, and a high stopping power for gamma-rays due to their thick high- $Z$  materials ( $Z_{\text{eff}} = 71$ ). Figure 2 shows the effective area of the Anti units compared with those of other gamma-ray burst instruments, such as *Swift*/BAT, *CGRO*/BATSE, *HETE-2*/FREGATE, and *GLAST*/GBM. In the energy range of 300 keV to 5 MeV, the WAM thus has the largest effective area that has ever been achieved by gamma-ray instruments with nearly all-sky coverages. The WAM electronics are designed to acquire wide band energy spectra from 50 keV to 5 MeV.

Photons detected by the WAM are pulse-height analyzed into 55 energy channels covering 50 to 5000 keV, with a time resolution of 1 second. Figure 3 shows energy spectra of the WAM when irradiated by various radio isotopes in the preflight calibration. It clearly shows the photo-peaks at 59.5 keV from  $^{241}\text{Am}$  and 81 keV from  $^{133}\text{Ba}$ . The lower-energy threshold can be lowered down to  $\sim 30$  keV. The typical energy resolution of the WAM is  $\sim 30\%$  at 662 keV. A background spectrum obtained in the preflight calibration is also shown in fig. 3 with circles; there are also peaks at 1.46 MeV from the environmental  $^{40}\text{K}$  and at 2.6 MeV from  $^{208}\text{Tl}$ .

### 3. – GRB observation with the WAM

**3.1. Detection.** – The detection of gamma-ray bursts (GRBs) is achieved by monitoring the WAM count rates. The automated burst detection algorithm, designed based on the Gamma-ray Burst Detector (GBD) on *Ginga* satellite [6], utilizes both hardware circuits and the onboard software. This algorithm utilizes a criterion as  $\frac{S\Delta t}{m} - \frac{B\Delta t}{m} > \sigma\sqrt{\frac{B\Delta t}{m}}$ , where  $S$  and  $B$  are the source and background rates,  $\Delta t$  is the integration time (1/4 or 1 s), and  $m$  is the judge level factor ( $m = 1, 2, 4, 8$ ). Table I shows a summary of the burst detection function of the WAM. Once a GRB is detected, the data are acquired both before 16 seconds and after 112 seconds of the burst using a ring buffer. These data are obtained in 4 energy bins (roughly 50–100 keV, 100–250 keV, 250–500 keV, and 500 keV–5 MeV) with a time resolution of 1/32 seconds. However, a real time alert is not issued, since the satellite has no data link except the ground tracking station in Japan. The GRB location will be determined with an accuracy of 5 degrees, in a ground analysis using count rate ratios among units.

**3.2. Estimation of detection rate.** – The overall GRB occurrence rate is assumed to be 666 per one year from the revised fourth BATSE GRB catalog [7]. The WAM in-orbit background rate is estimated to be 2–10 kHz for one side. Although the field of view of the WAM is about  $2\pi$ , the Earth hides  $0.8\pi$  of that. So, the field of view of the WAM is 30% of the all sky. Considering these factors, the WAM is expected to detect 100–60 GRBs each year with  $10\sigma$  detection thresholds.

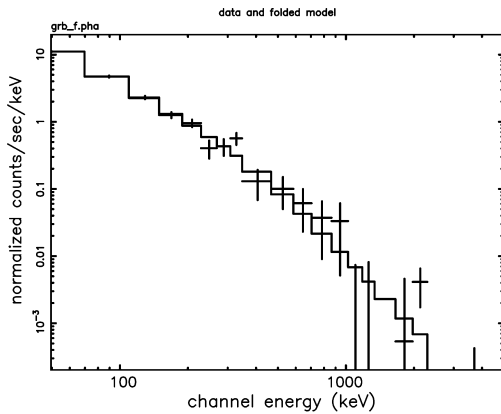


Fig. 4

Fig. 4. – A simulated WAM spectrum of a GRB.

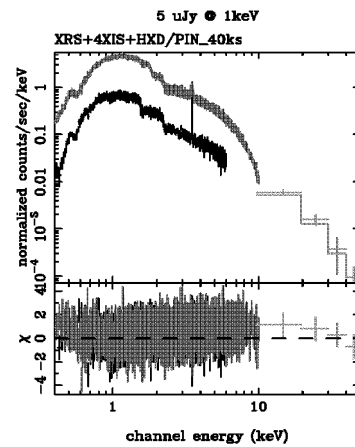


Fig. 5

Fig. 5. – A simulated 1 day afterglow spectrum of GRB030329, for a 40 ks exposure.

**3.3. Spectrum simulation.** – A detector simulator of the HXD-II is being developed. It employs a response matrix, generated by a Monte Carlo Method using the GEANT4 [5, 8]. Figure 4 shows a simulated spectrum of a GRB by the WAM using this response matrix. It assumes typical GRB parameters from the BATSE ( $\alpha = -1.3$ ,  $\beta = -2.3$ ,  $E_p = 200$  keV, duration = 20 s) [7] and a flux of 1 photons/cm<sup>2</sup>/s at 50–300 keV. Thus, the WAM will acquire GRB spectra over an energy range from 50 keV to a few MeV.

**3.4. Afterglow spectra by *Astro-E2*.** – Figure 5 shows a simulated GRB afterglow spectrum detected by *Astro-E2*. Assuming the 1 day afterglow emission from GRB030329, the HXD Well units will be able to detect the emission up to  $\sim 50$  keV. Furthermore, the two focal plane instruments (the XRS and the XIS) will detect lower energy signals with superior statistics. An iron line with an equivalent width of  $\sim 100$  eV will be detected up to a redshift of  $z \sim 1$ .

#### 4. – Conclusion

The HXD-II Anti units, or the WAM, have three characteristics; a wide field of view ( $\sim 2\pi$ ), a large effective area (400 cm<sup>2</sup> at 1 MeV), and a wide energy band (50 keV to 5 MeV). Utilizing these properties, the WAM is expected to detect 60–100 GRBs per year, and acquire wide band energy spectra in the energy range of 50 keV to 5 MeV. The GRB locations will be determined with an accuracy of 5 degrees. The *Astro-E2* satellite is ready for launch, which will take place in the summer of 2005.

#### REFERENCES

- [1] TASHIRO M. *et al.*, *IEEE Trans. Nucl. Sci.*, **49** (2002) 1893.
- [2] KOKUBUN M. *et al.*, *IEEE Trans. Nucl. Sci.*, **51** (2004) 1991.
- [3] KAWAHARADA M. *et al.*, *Proc. SPIE*, **5501** (2004) 286.
- [4] YAMAOKA K. *et al.*, submitted to *IEEE Trans. Nucl. Sci.*, (2005).
- [5] OHNO M. *et al.*, submitted to *IEEE Trans. Nucl. Sci.*, (2005).
- [6] MURAKAMI T. *et al.*, *PASJ*, **41** (1989) 405.
- [7] PACIASAS W. S. *et al.*, *ApJS*, **122** (1999) 465.
- [8] TERADA Y. *et al.*, to be published in *IEEE Trans. Nucl. Sci.*, (2005).